Table 2. Characteristics of the 5-year survivors

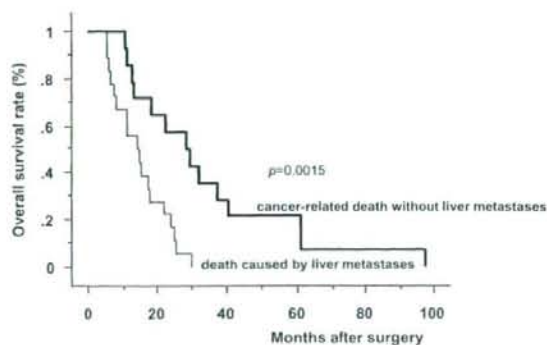|	Age (years)	Sex	T category	N category	Stage	Outcome
1.	60	Female	t3	n1	III	Dead (61.0 months; local recurrence)
2.	58	Male	t4	n1	IVa	Dead (61.0 months; pleural dissemination)
3.	71	Female	t3	n1	III	Alive (95.4 months)
4.	66	Male	t3	n2	IVa	Dead (97.9 months; lung metastases)
5.	56	Female	t3	n1	III	Dead (164 months; renal failure)
6.	37	Female	t2	n0	II	Alive (254.5 months)

Table 3. Outcomes after extended radical resection combined with IORT for patients with pancreatic cancer

	No.	Survival time in months; median (range)
Cancer-related death	32	
Liver metastases	18	14.3 (5.6–30)
Without liver metastases	14	28.4 (10.8–97.7)
Lung metastases	3	
Peritoneal dissemination	6	
Pleural dissemination	1	
Recurrence in remnant pancreas	2	
Local recurrence	2	
Non-cancer-related death	7	
Hospital death (intraperitoneal bleeding)	4	2.2 (1.6–8.3)
Non-hospital death	3	32 (8.3–164)
Malnutrition	1	
Cardiac failure	1	
Renal failure	1	
Alive	2	

IORT, intraoperative radiation therapy

No. at Risk   41   24   6   4   2   2
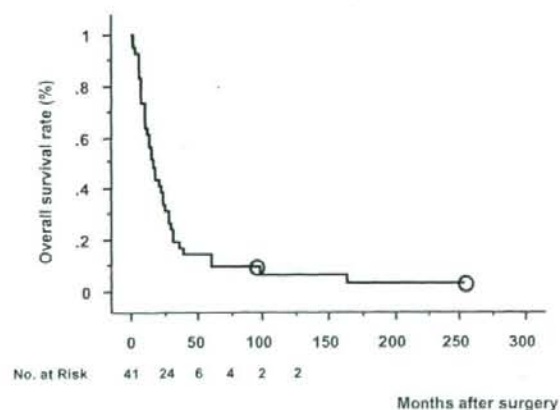
Fig. 1. The cumulative survival curve in this series is depicted; the curve was constructed using the Kaplan-Meier method

Fig. 2. Survival rates in the 32 patients who died of cancer-related causes, comparing patients with liver metastases and patients with other recurrences

14 patients without liver metastases died between 10.8 and 97.7 months after the surgery. Hospital death caused by intraabdominal bleeding occurred from 1.6 to 8.3 months after surgery in 4 patients (9.8%). The patients who experienced liver metastases had a median survival time of 14.3 months, and they had a significantly worse prognosis than those with other cancer-related causes of death (median survival time, 28.4 months; Fig. 2). The patients with stage IV disease had a significantly worse prognosis than those with stage II or III (Fig. 3). R0 resection did not contribute to survival benefit compared with R1-2. The pl (+) group had a significantly poorer prognosis compared with the pl (−) group
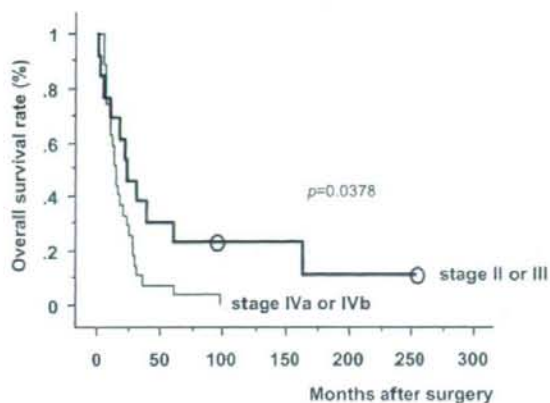
Fig. 3. Kaplan-Meier analysis of survival according to stage

Fig. 5. Kaplan-Meier analysis of survival according to lymp node metastases (n)
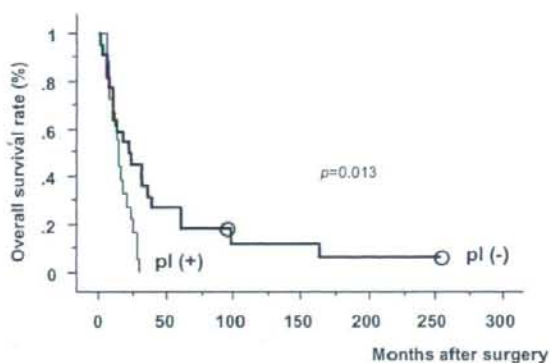

Fig. 4. Kaplan-Meier analysis of survival according to extra-pancreatic nerve plexus invasion (*pl*)

(Fig. 4). No significant difference in survival was observed between the pv (+) and pv (−) groups. The patients with n3 had a significantly worse prognosis than the others (Fig. 5), although there was no significant difference in survival between the n (−) and n (+) groups, or between the n0-1 and n2-3 groups.

Discussion

Several studies have revealed that pancreatic resection can yield actual 5-year survival rates of 15% to 25% following pancreaticoduodenectomy and 8%–14% following distal pancreatectomy for PC. The patients with PC who received the combined therapy in the present study had an actual 5-year survival rate of 14.6%, and the therapy provided no survival benefit. Two random-ized trials have shown that there was no survival benefit from extended surgery compared with a standard oper-
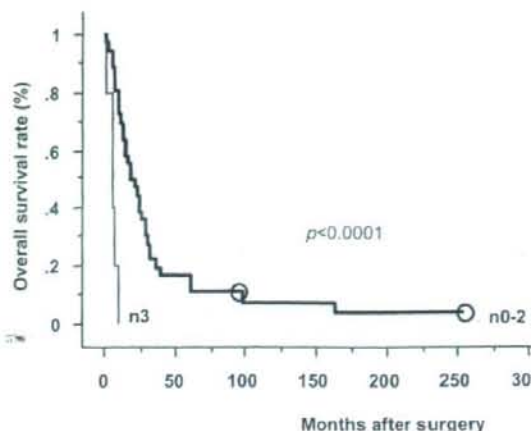
ation,[10,11] although several retrospective reports fro Japan showed that extended surgery might have a su vival benefit for patients with operable PC.[12-14] On tl other hand, Pawlik et al.[15] stated that adequate powered randomized trials to address the potenti benefit of extended lymphadenectomy would not l feasible, because these would require a prohibitive large sample size.

We have reported previously that the combin therapy we have described here diminished loc relapses, compared with standard resections alor although it has not contributed to improving survival Other studies have also shown that IORT has lit impact on survival, compared with surgery alone.[16-18] the present long-term follow-up study, local recurren was observed in only 2 patients (5.0%), although autc sies disclosed microscopic local recurrence in 4 (28.6° of the 14 patients. The usefulness of imaging studies l the diagnosis of local relapse may be limited, becau in some cases, cancer cells may infiltrate the retrope toneal soft tissue in the radiation field without the f mation of a mass.[18] In the present study, we found th histologically, these microscopic local relapses consist of small numbers of cancer cells within surroundi thick connective tissue at autopsy (data not show These local recurrences seem to be a direct cause death, as Hishinuma et al.[18] have mention previously.

One of our interesting findings was that the patie who died of liver metastases had a significantly wo prognosis than those who had other recurrence p terns. In an analysis of the cumulative survival curve PC, we reported that the early postoperative phi reflected the poor prognosis of patients who died hepatic metastases.[19] Raut et al.[4] have mentioned tl

subclinical metastases are present in most patients at the time of diagnosis, even when imaging studies are normal. Therefore, more precise diagnostic tools for liver metastases and a strategy to prevent the formation of liver metastases are required to improve the survival of PC patients with resectable disease. We have proposed the diagnostic advantage of computed tomography during arterial portography, combined with computed tomography-assisted hepatic arteriography (CTAP + CTHA) for the preoperative detection of liver metastases secondary to PC.[20] CTAP + CTHA should be performed to select resectable PC before surgery.

In the present study, the pl (+) and n3 groups had significantly poorer prognoses than the other patients. These conditions may have reflected systemic spread rather than localized disease, because pl (+) was reported to be one of the most powerful predictive factors of liver metastases.[21] Several reports have shown that the R factor is one of the highly significant prognostic factors after resection for PC.[22-24] Interestingly, in the present study, the R1 and R2 groups did not have significantly poorer survival compared with the R0 group. It is unclear whether pv is a prognostic factor after surgery.[25] Our results showed no significant difference in survival between the pv (+) and pv (−) groups.

In conclusion, the combined therapy used in the present study improved local control; however, it provided no survival benefit for resectable PC, because of liver metastases. This combined therapy might be reassessed, if a strategy to prevent liver metastases is to be established in future.

References

1. Rockhart AC, Rothenberg ML, Berlin JD. Treatment for pancreatic cancer: current therapy and continued progress. Gastroenterology 2005;128:1642–54.
2. Griffin JF, Smally SR, Jewell W, Paradelo JC, Reymond RD, Hassancin RE, et al. Patterns of failure after curative resection of pancreatic carcinoma. Cancer 1990;66:56–61.
3. Sperti C, Pasquali C, Piccoli A, Pedrazzoli S. Recurrence after resection for ductal adenocarcinoma of the pancreas. World J Surg 1997;21:195–200.
4. Raut CP, Evans DB, Crane CH, Pisters PW, Wolff RA. Neoadjuvant therapy for pancreatic cancer. Surg Oncol Clin N Am 2004;13:639–61.
5. Hiraoka T, Kanemitsu K. Treatment using combined modalities. In: Howard JM, editor. Surgical diseases of the pancreas. Bartimore: Williams & Wilkins; 1988. p. 605–11.
6. Hiraoka T, Nakamura I, Tashiro S, Miyauchi Y. Intraoperative radiation therapy for pancreatic cancer in Japan. In: Dobelbower RR Jr, Abe M, editors. Intraoperative radiation therapy. Boca Raton, Florida: CRC; 1989. p. 181–93.
7. Hiraoka T, Watanabe E, Mochinaga M, Tashiro S, Miyauchi Y, Nakamura I, et al. Intraoperative radiation combined with radical resection for cancer of the head of the pancreas. World J Surg 1984;8:766–71.
8. Cubilla AL, Fortner J, Fitzgerald PJ. Lymph node involvement in carcinoma of the head of the pancreas. Cancer 1978;41:880–7.
9. Japan Pancreas Society. Classification of pancreatic cancer. Second English ed. Tokyo: Kanehara; 2003. p. 4–12.
10. Pedrazzoli S, DiCarlo V, Dionigi R, Mosca F, Pederzoli P, Pasquali C, et al. Standard versus extended lymphadenectomy associated with pancreatoduodenectomy in the surgical treatment of adenocarcinoma of the head of the pancreas: a multicenter, prospective, randomized study. Lymphadenectomy Study Group. Ann Surg 1998;228:508–7.
11. Yeo CJ, Cameron JL, Sohn TA, Coleman J, Sauter PK, Hruban RH, et al. Pancreaticoduodenectomy with or without extended retroperitoneal lymphadenectomy for periampullary adenocarcinoma: comparison of morbidity and mortality and short-term outcome. Ann Surg 1999;229:613–24.
12. Ishikawa O, Ohhigashi H, Sasaki Y, Kabuto T, Fukuda I, Furukawa H, et al. Practical usefulness of lymphatic and connective tissue clearance for the carcinoma of the pancreas head. Ann Surg 1988;208:215–20.
13. Manabe T, Ohshio G, Baba N, Miyashita T, Asano N, Tamura K, et al. Radical pancreatectomy for ductal cell carcinoma of the head of the pancreas. Cancer 1989;64:1132–7.
14. Hiraoka T, Uchino R, Kanemitsu K, Toyonaga M, Saitoh N, Nakamura I, et al. Combination of intraoperative radiation with resection of cancer of the pancreas. Int J Pancreatol 1990;7: 201–7.
15. Pawlik TM, Abdolla EK, Barnett CC, Ahmad SA, Cleary KR, Vauthey JN, et al. Feasibility of a randomized trial of extended lymphadenectomy for pancreatic cancer. Arch Surg 2005;140: 584–91.
16. Wagman R, Grann A. Adjuvant therapy for pancreatic cancer. Current treatment approaches and future challenges. Surg Clin North Am 2001;81:667–81.
17. Sumanura M, Kobari M, Lozonschi L, Egawa S, Matsuno S. Intraoperative radiotherapy for pancreatic adenocarcinoma. J Hepatobiliary Pancreat Surg 1998;5:151–6.
18. Hishinuma S, Ogata Y, Matsui J, Ozawa I. Results of surgery and adjuvant radiotherapy for pancreatic cancer. J Hepatobiliary Pancreat Surg 1998;5:143–50.
19. Takamori H, Hiraoka T, Kanemitsu K, Tsuji T, Hamada C, Baba H. Identification of prognostic factors associated with early mortality after surgical resection for pancreatic cancer. Under analysis of cumulative survival curve. World J Surg 2006;30:213–8.
20. Takamori H, Ikeda O, Kanemitsu K, Tsuji T, Chikamoto A, Kusano S, et al. Preoperative detection of liver metastases secondary to pancreatic cancer. Utility of combined helical computed tomography during arterial portography with biphasic computed tomography-assisted hepatic arteriography. Pancreas 2004;29:188–92.
21. Takamori H, Hiraoka T, Kanemitsu K, Tsuji T. Pancreatic liver metastases after curative resection combined with intraoperative radiation for pancreatic cancer. Hepatogastroenterology 2004;51: 1500–3.
22. Yeo CJ, Cameron JL, Lillemore KD, Sitzmann JV, Hruban RH, Goodman SN, et al. Pancreaticoduodenectomy for cancer of the head of the pancreas: 201 patients. Ann Surg 1995;221:721–33.
23. Millikan KW, Deziel DJ, Silverstein JC, Kanjo TM, Christein JD, Doolas A, et al. Prognostic factors associated with resectable adenocarcinoma of the head of the pancreas. Am Surg 1999; 65:618–23.
24. Benassai G, Mastrorilli M, Quarto G, Cappiello A, Giani U, Forestieri P, et al. Factors influencing survival after resection for ductal adenocarcinoma of the head of the pancreas. J Surg Oncol 2000;73:212–8.
25. Nakagohri T, Kinoshita T, Konishi M, Inoue K, Takahashi S. Survival benefits of portal vein resection for pancreatic cancer. Am J Surg 2003;186:149–53.

Characterization of heparan sulfate on hepatocytes in regenerating rat liver

Akitoshi Kimura, Yoshikazu Toyoki, Kenichi Hakamada, Shuichi Yoshihara, and Mutsuo Sasaki

Department of Surgery, Hirosaki University Graduate School of Medicine, 5 Zaifu-cho, Hirosaki 036-8562, Japan

Abstract

Background/Purpose. Liver regeneration occurs through interactions between the receptors on hepatocytes, including proteoglycans (PGs) and glycosaminoglycans (GAGs), and various growth factors. We investigated serial changes in GAGs, particularly heparan sulfate (HS), in proliferating hepatocytes.

Methods. We performed 70% hepatectomy in male Wistar rats, and we then isolated hepatocytes by a collagenase perfusion method after each surgery. DNA synthesis was evaluated by measuring proliferating cell nuclear antigen (PCNA). After we had treated the hepatocytes by delipidation and digestion with actinase E, endo-β-xylosidase, and α-amylase, we quantified GAGs by a carbazole-sulfuric acid method. GAGs were analyzed by ion-exchange chromatography, and changes in molecular weight of the HS component were investigated by size-fractionation HPLC.

Results. Hepatocyte mitosis peaked at 24 h after the amount of GAGs was increased at 24 and 72 h after surgery. The amount of HS was slightly increased at 3 to 12 h after surgery, and then peaked at 24 h. The molecular weight of the HS declined by 12 h, but had recovered to the preoperative level by 24 h.

Conclusions. These results suggested that this HS molecule, which contained about ten disaccharide units during proliferation, may be an initiator of hepatocyte proliferation.

Key words Liver regeneration · DNA synthesis · Proteoglycan · Glycosaminoglycan

but only limited data are available on the relationship between the mechanism of regeneration and the activity of proteoglycans (PGs) and/or glycosaminoglycans (GAGs) on hepatocytes.[1–13] Moreover, several cytokines and growth factors that start and stop hepatocyte proliferation, such as hepatocyte growth factor (HGF) and tumor necrosis factor α (TNF-α) are correlated with PGs and/or GAGs.[2–5,7,10,12–21] HGF and the MET receptor activate the G_1/S phase of hepatocyte growth after partial hepatectomy.[7,8] Also, epidermal growth factor (EGF) is involved with the continuation of the G_1/S phase.[7,8] HGF binds the MET receptor, and the complex unit binds with heparan sulfate proteoglycan (HS-PG).[2] Similarly, the EGF family binds with EGF receptors, and this unit binds with HS-PG, too.[19–21] PGs and GAGs have been demonstrated in regenerating liver tissue by biochemical and immunohistochemical techniques.[22–26] However, few reports have focused on PGs and/or GAGs on hepatocytes in regenerating liver tissue. Previously, we reported on GAGs in regenerating canine liver tissue.[27] We observed transient changes in HS with a decreased chain length observed during liver regeneration.

In the present study, we investigated the properties of GAGs on hepatocytes in the regenerating rat liver after partial (70%) hepatectomy; to our knowledge, this study is the first investigation of GAGs on proliferating hepatocytes in vivo.

Introduction

The liver is a living organ that has a high capacity for regeneration. Many reports have revealed that some cytokines and growth factors control liver regeneration,

Materials and methods

Chemicals

Collagenase type IV, trypsin inhibitor, albumin from bovine serum (BSA), Hanks solution, phenylmethylsulfonyl fluoride (PMSF), pepstatin A, and leupeptin were purchased from Sigma Chemical (Tokyo, Japan). Actinase E was obtained from Kaken Pharmaceutical

Involvement of autophagy in trypsinogen activation within the pancreatic acinar cells

Daisuke Hashimoto,[1,2] Masaki Ohmuraya,[1,2] Masahiko Hirota,[2] Akitsugu Yamamoto,[3] Koichi Suyama,[1,2] Satoshi Ida,[1,2] Yuushi Okumura,[4,5] Etsuhisa Takahashi,[5] Hiroshi Kido,[5] Kimi Araki,[1] Hideo Baba,[2] Noboru Mizushima,[6,7] and Ken-ichi Yamamura[1]

[1]Division of Developmental Genetics, Institute of Molecular Embryology and Genetics, and [2]Department of Gastroenterological Surgery, Kumamoto University, Kumamoto 860-0811, Japan
[3]Department of Bioscience, Nagahama Institute of Bioscience and Technology, Nagahama, Shiga 526-0829, Japan
[4]Department of Nutritional Physiology, Institute of Health Biosciences, and [5]Division of Enzyme Chemistry, Institute for Enzyme Research, University of Tokushima Graduate School, Tokushima 770-8503, Japan
[6]Department of Physiology and Cell Biology, Tokyo Medical and Dental University, Bunkyo-ku, Tokyo 113-8519, Japan
[7]Solution Oriented Research for Science and Technology, Japan Science and Technology Agency, Kawaguchi, Saitama 332-0012, Japan

Autophagy is mostly a nonselective bulk degradation system within cells. Recent reports indicate that autophagy can act both as a protector and killer of the cell depending on the stage of the disease or the surrounding cellular environment (for review see Cuervo, A.M. 2004. *Trends Cell Biol.* 14:70–77). We found that cytoplasmic vacuoles induced in pancreatic acinar cells by experimental pancreatitis were autophagic in origin, as demonstrated by microtubule-associated protein 1 light chain 3 expression and electron microscopy experiments. To analyze the role of macroautophagy in acute pancreatitis, we produced conditional knockout mice lacking the *autophagy-related 5* gene in acinar cells. Acute pancreatitis was not observed, except for very mild edema in a restricted area, in conditional knockout mice. Unexpectedly, trypsinogen activation was greatly reduced in the absence of autophagy. These results suggest that autophagy exerts devastating effects in pancreatic acinar cells by activation of trypsinogen to trypsin in the early stage of acute pancreatitis through delivering trypsinogen to the lysosome.

Introduction

There are at least three types of autophagy: (1) macroautophagy, (2) chaperone-mediated autophagy, and (3) microautophagy (Mizushima, 2005). Although autophagy is mostly a nonselective bulk degradation system within cells, chaperone-mediated autophagy is a selective degradation system in which cytoplasmic proteins are refolded and transported into the lysosome lumen across the membrane (for review see Cuervo, 2004). In microautophagy, only a small portion of cytoplasm is taken up directly by invagination of lysosome membrane into the lumen. As macroautophagy is believed to be the primary means for cytoplasm to lysosome delivery, it is most commonly referred to simply as autophagy. Genetic studies on yeast have identified >20 *autophagy-related* (*ATG*) genes that are required for autophagosome formation (Klionsky et al., 2003; Klionsky, 2005).

Autophagy-defective yeast mutants are not able to survive during nitrogen starvation (Tsukada and Ohsumi, 1993). Similarly, most of the Atg5^{−/−} and Atg7^{−/−} mice died within 1 d after birth (Kuma et al., 2004; Komatsu et al., 2005). Thus, autophagy is thought to be important for the cellular response to starvation and the normal turnover of cytoplasmic constituents.

Acute pancreatitis has long been considered to be an autodigestive disorder in which inappropriate activation of trypsinogen to trypsin within pancreatic acinar cells leads to the development of pancreatitis (Hirota et al., 2006). However, the mechanisms responsible for intracellular activation of trypsin have not been elucidated with certainty. There are two major hypotheses: the colocalization hypothesis (van Acker et al., 2006) and the autoactivation hypothesis (Leach et al., 1991). According to the former hypothesis, digestive enzymes become colocalized with lysosomal hydrolases, such as cathepsin B, and activate trypsinogen in cytoplasmic vacuoles of acinar cells (Steer and Meldolesi, 1987). The latter hypothesis suggests that trypsinogen is autoactivated under low pH conditions in the presence of serine protease (Leach et al., 1991). However, the mode of trypsinogen

D. Hashimoto and M. Ohmuraya contributed equally to this paper.

Correspondence to Ken-ichi Yamamura: yamamura@gpo.kumamoto-u.ac.jp

Abbreviations used in this paper: Atg, autophagy related; CCK, cholecystokinin; H&E, hematoxylin and eosin; LC3, light chain 3; TAP, trypsinogen activation peptide.

The online version of this article contains supplemental material.

Figure 1. **Autophagy induction in pancreatic acinar cells of cerulein-induced acute pancreatitis.** Overnight-starved mice were treated by saline (A) or cerulein 6 (B), 9 (C), or 12 (D) times, and pancreatic sections were analyzed by H&E staining. Insets show higher magnifications of areas indicated in A–D. (E) Serum amylase activity in mice with cerulein-induced pancreatitis. Data are shown as mean ± SEM (error bars). *, $P < 0.05$. Bars, 50 µm.
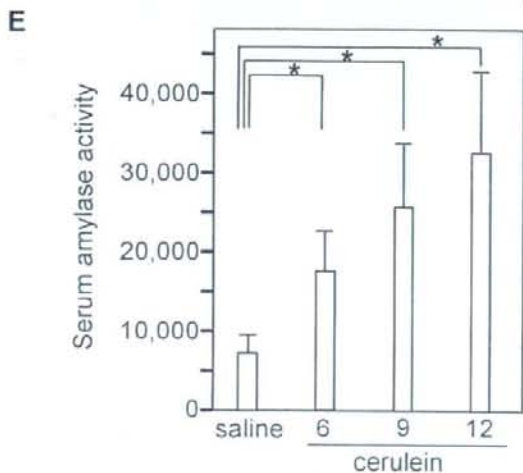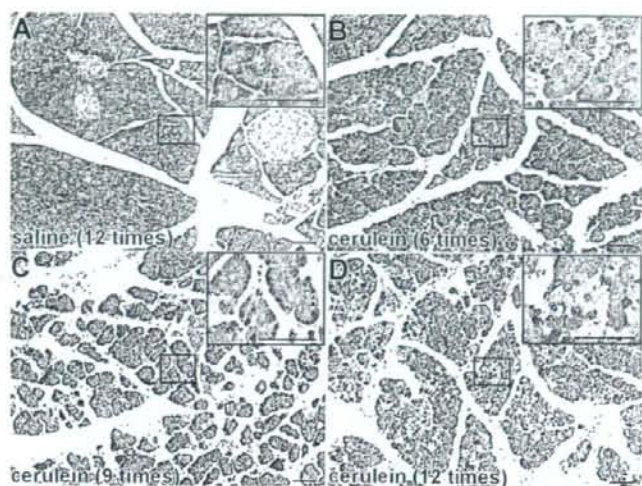
delivery to the lysosomes or cellular compartments has been the subject of investigation. There are three possible mechanisms for delivery of trypsinogen to the cellular compartment where activation occurs. One is fusion of zymogen granules with lysosomes (crinophagy; Koike et al., 1982). The second is perturbation of normal intracellular trafficking of zymogen granules and lysosomal hydrolases. The third is endocytic vacuole formation through uptake of secreted digestive enzymes by acinar cells via endocytosis, transportation to endosomes, and fusion of endosomes with lysosomes (Sherwood et al., 2007). One important clue to distinguish between these possibilities is the appearance of cytoplasmic vacuoles within pancreatic acinar cells (Watanabe et al., 1984). This is an early feature of acute pancreatitis. EM and immunohistochemical studies suggested that many vacuoles observed in both experimental and human acute pancreatitis were autophagic in origin (Helin et al., 1980; Adler et al., 1985). Our previous study suggested that autophagy was induced in the

acinar cells of mice with experimental pancreatitis induced by cerulein (cholecystokinin [CCK] analogue; Ohmuraya et al., 2005). Collectively, these results indicate that vacuoles are autophagic in origin and that autophagy is somehow involved in the development of pancreatitis.

In this study, we report that cytoplasmic vacuoles induced in experimental acute pancreatitis are autophagic in origin and that absence of autophagy in the *Atg5* conditional knockout mouse results in greatly reduced acute pancreatitis caused by loss of trypsinogen activation in pancreatic acinar cells. Our results suggest that trypsinogen is delivered to the endosome or lysosome through autophagosome/autolysosome formation.

Results and discussion

We first analyzed the origin of vacuoles in cerulein-induced experimental pancreatitis. No changes in pancreatic morphology
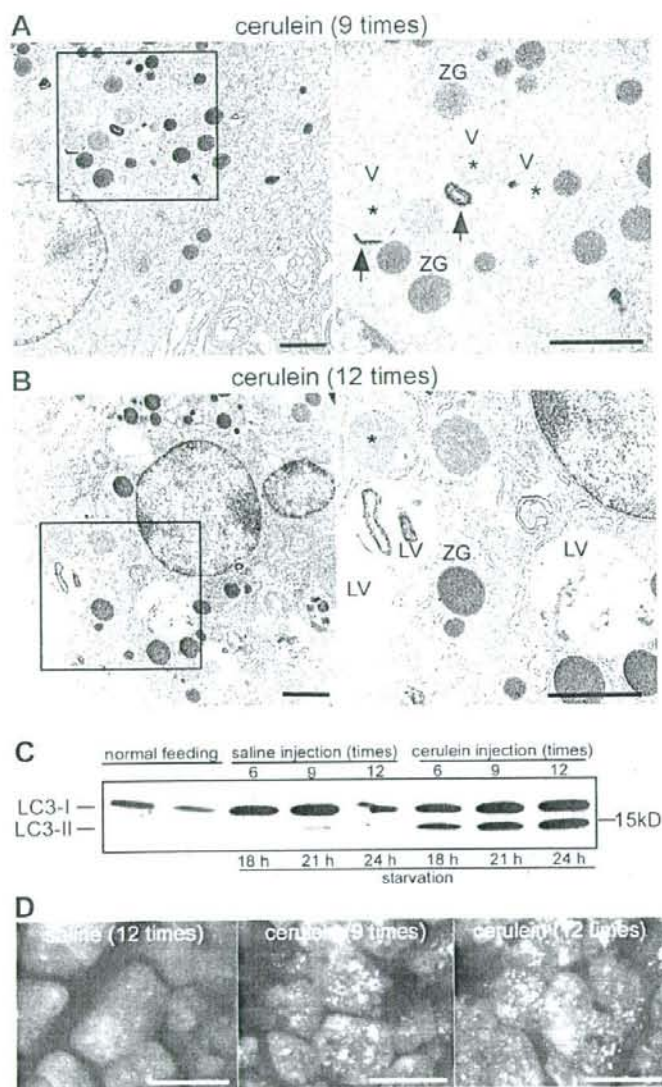
A cerulein (9 times)

ZG

V

V

V

*

*

ZG

B cerulein (12 times)

*

LV ZG

LV

LV

LV

C

normal feeding   saline injection (times)   cerulein injection (times)

6   9   12   6   9   12

LC3-I —
LC3-II —   —15kD

18 h   21 h   24 h   18 h   21 h   24 h

starvation

D

saline (12 times)   cerulein (9 times)   cerulein (12 times)

Figure 2. **Appearance of autophagic vacuoles in cerulein-induced pancreatitis.** (A and B) Mice were injected with cerulein 9 (A) or 12 (B) times, and the pancreas was analyzed by EM. The right panels show higher magnification of the boxed areas. V, autophagic vacuole; ZG, zymogen granule; asterisk, zymogen granule contained in vacuole; arrow, membrane-bound organelle contained in vacuole; LV, large vacuole. (C) LC3 conversion in acute pancreatitis. Pancreas homogenates were prepared from cerulein-injected mice and subjected to immunoblotting using anti-LC3 antibody. The cytosolic LC3-I protein (16 kD) was converted into LC3-II (14 kD), and the amount of LC3-II was correlated with the extent of autophagosome formation. (D) GFP-LC3 mice were treated with cerulein and analyzed by fluorescence microscopy. Bars: (A and B) 2 μm; (D) 10 μm.

were observed at any time in any sample obtained from saline-injected mice (Fig. 1 A). In contrast, acute pancreatitis was observed in cerulein-injected mice. The severity of acute pancreatitis increased with the number of cerulein injections. With six and nine cerulein injections, mild edema and acinar cell degeneration were observed (Fig. 1, B and C). With 12 cerulein injections, the pancreas showed severe acinar cell degeneration with significant edema and inflammatory cell infiltration in the interstitium (Fig. 1 D). In accordance with histological changes, we observed a significant increase in serum amylase activity (Fig. 1 E). The observed increase was proportional to the cerulein dose and the severity of acute pancreatitis. To examine the induction of

autophagy, we performed EM examination, which revealed vacuoles containing zymogen granules (Fig. 2 A, asterisks) in acinar cells after nine cerulein injections (Fig. 2 A). Some vacuoles contained both zymogen granules and membrane-bound organelles (Fig. 2 A, arrows), suggesting nonselective uptake. EM images after 12 cerulein injections were characterized by an increase in vacuoles containing zymogen granules and organelles and by the appearance of large vacuoles with homogeneous material that seemed to be autolysosomes (Fig. 2 B). There are two forms of microtubule-associated protein 1 light chain 3 (LC3), a mammalian homologue of yeast Atg8. LC3-I is localized in the cytoplasm and is converted into LC3-II, which is associated with the
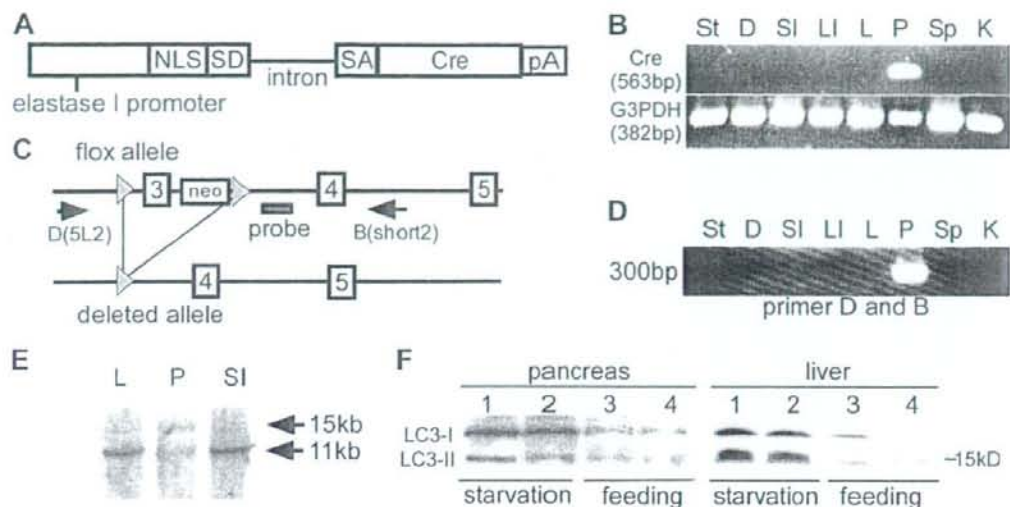
Figure 3. **Establishment of EL-Cre transgenic mouse.** (A) Structure of the EL-Cre gene. NLS, nuclear localization signal domain; SD, splice donor; SA, splice acceptor; Cre, Cre recombinase; pA, polyadenylation signal. (B) RT-PCR analysis detecting Cre recombinase in each organ at 2 mo of age. (C) The deletion of exon 3 flanked by loxP in the flox allele by Cre recombinase results in a loss of function mutation. (D) PCR analysis showing the 300-bp band lacking exon 3 only in the pancreas, not in the stomach, intestine, liver, spleen, and kidney. (E) Southern blot analysis showing the presence of two bands, the 15-kb deleted allele and 11-kb wild allele. (F) Western blot analysis of LC3 in the pancreas and liver in $Atg5^{flox/flox}$ mice (lanes 1 and 3) and $Atg5^{flox/flox}$; EL-Cre2 mice (lanes 2 and 4). Mice were starved for 24 h and examined for induction of autophagy. St, stomach; D, duodenum; SI, small intestine; LI, large intestine; L, liver; P, pancreas; Sp, spleen; K, kidney.

autophagosome membrane in a phosphatidylethanolamine-conjugated form (Ichimura et al., 2000; Kabeya et al., 2000). The amount of LC3-II is thus correlated with the extent of autophagosome formation. In control mice, LC3-II was increased slightly by starvation but was virtually unchanged during saline treatment (Fig. 2 C). In mice treated with cerulein, a dose-dependent increase in LC3-II level was observed. Autophagy can also be monitored by detection of GFP fluorescence in GFP-LC3 mice (Mizushima et al., 2004). After 24-h fasting, some dots that represent autophagosomes were detected in the cytoplasm in saline-injected mice (Fig. 2 D). After cerulein injection, many dots were observed, and the number of GFP-LC3 dots from mice receiving 12 cerulein injections was larger than from mice with nine cerulein injections (Fig. 2 D). Together with EM examination, these results suggest that vacuoles are autophagic in origin.

To analyze the role of autophagy in acute pancreatitis, we established conditional knockout mice in which the *Atg5* gene was deleted in pancreatic acinar cells. We obtained an EL (rat *elastase I* promoter/enhancer)-*Cre* mouse line (EL-*Cre2*) in which *Cre* was specifically expressed in the pancreas under the control of EL (Fig. 3, A and B). This line was crossed with $Atg5^{flox/flox}$ (Hara et al., 2006) to produce $Atg5^{flox/flox}$;EL-*Cre2* mice (Fig. 3 C). *Cre*-mediated excision of exon 3 of the *Atg5* gene was detected in the pancreas but not in other organs of $Atg5^{flox/flox}$;EL-*Cre2* (Fig. 3 D). Southern blot analysis using genomic DNA from the pancreas showed that recombination occurred in about half of the pancreatic cells (Fig. 3 E). As the pancreas contains not only acinar cells but also endocrine and duct cells, this ratio suggests that recombination occurred in most $Atg5^{flox}$ alleles of the acinar

cells. The expression of *Cre* in acinar cells was also assessed by expression of *lacZ* in mice obtained by mating EL-*Cre2* mice with a reporter line for monitoring Cre expression, R26R (Soriano, 1999). All acinar cells examined were stained with X-gal, suggesting that recombination occurred in all $Atg5^{flox}$ alleles of the acinar cells (unpublished data). To further demonstrate the inactivation of *Atg5* in acinar cells, we analyzed induction of autophagy under starving conditions. $Atg5^{flox/flox}$;EL-*Cre2* mice and $Atg5^{flox/flox}$ mice were starved for 24 h and examined for induction of autophagy. Autophagy was greatly induced in the liver and slightly induced in the pancreas of $Atg5^{flox/flox}$;EL-*Cre2* after starvation (Fig. 3 F). As *Atg5* was present in nonacinar cells, autophagy may be induced in these cells.

$Atg5^{flox/flox}$;EL-*Cre2* mice were born healthy with no signs of developmental anomalies and grew without displaying any noticeable pathological phenotype after 2 mo (Fig. S1, available at http://www.jcb.org/cgi/content/full/jcb.200712156/DC1). There were no apparent abnormalities in blood biochemistry, such as total protein, glucose, total cholesterol, amylase, and lipase (unpublished data). Hematoxylin and eosin (H&E) staining and EM analysis revealed that acinar cells were normal (Fig. S1, B and C). The levels of amylase and trypsinogen were the same in the pancreas of $Atg5^{flox/flox}$ and $Atg5^{flox/flox}$;EL-*Cre2* mice (Fig. S2). In addition, we examined whether the lack of *Atg5* affected CCK-induced calcium signaling in acinar cells. Type 2 and type 3 inositol 1,4,5-trisphosphate receptors (IP3R2 and IP3R3) are the major Ca²⁺ release channels responsible for secretagogue-induced Ca^{2+} signaling in pancreatic acinar cells (Futatsugi et al., 2005). Basal levels of IP3R1, -2, and -3 in both $Atg5^{flox/flox}$ and $Atg5^{flox/flox}$;El-*Cre2* mice at 2 mo of age
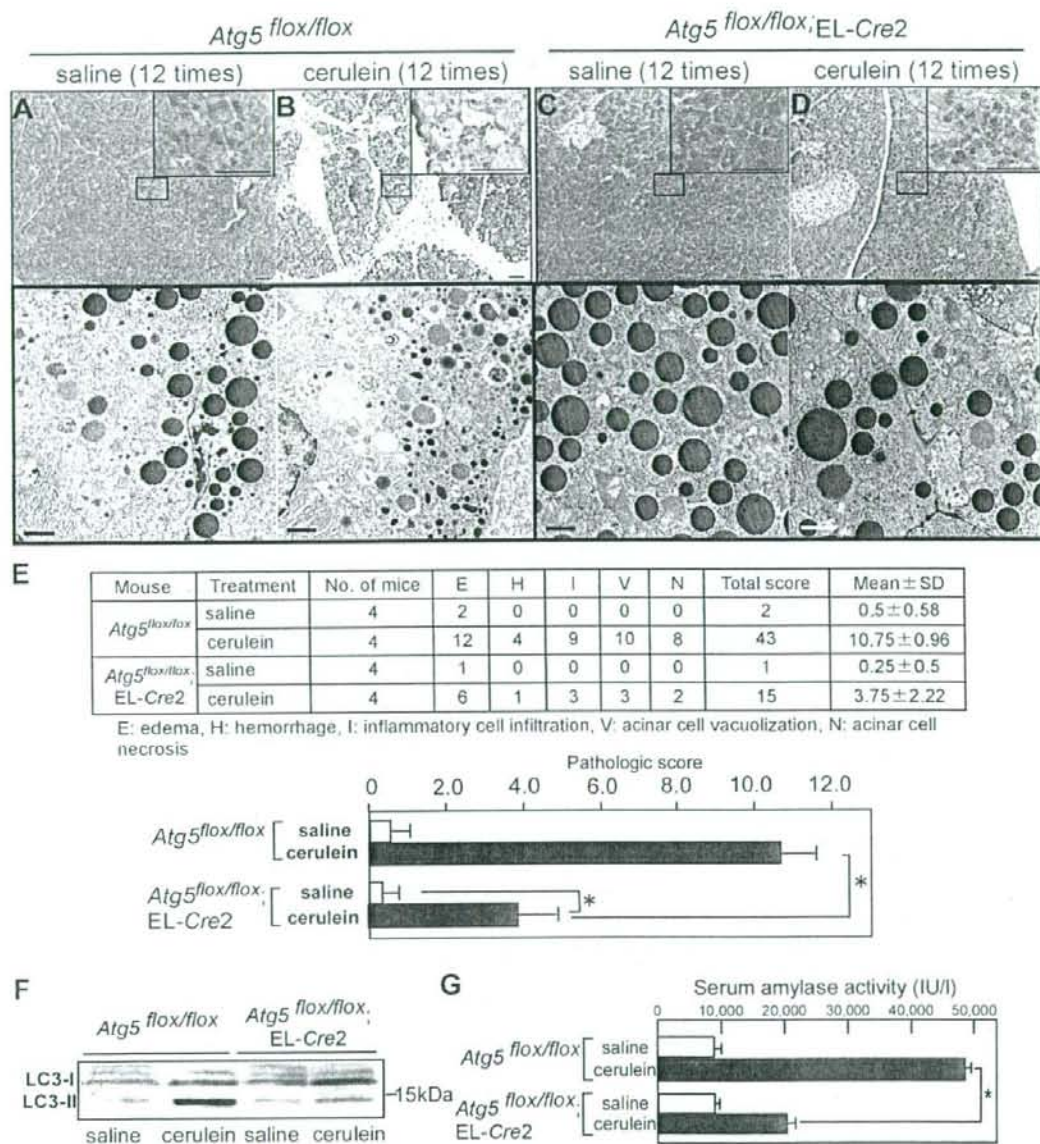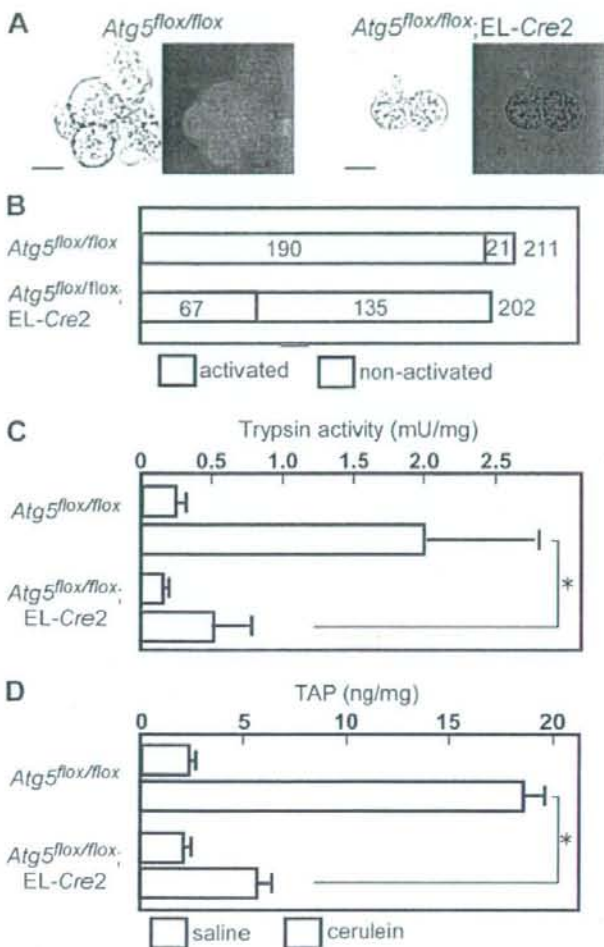
Figure 4. **Absence of cerulein-induced acute pancreatitis in acinar cell–specific Atg5-deficient mice.** *Atg5*^{flox/flox} (A and B) or *Atg5*^{flox/flox};EL-*Cre2* (C and D) mice were injected with saline or cerulein 12 times, and pancreatic sections were analyzed by H&E staining (A and C) and EM analysis (B and D). Insets show higher magnifications of areas indicated in A–D. EM analysis demonstrating the absence of autophagy in *Atg5*^{flox/flox};EL-*Cre2* mice. (E) Histological changes were quantified using a histological score by a pathologist. There was statistically significant difference in pathological changes between *Atg5*^{flox/flox} and *Atg5*^{flox/flox};EL-*Cre2* mice. Unpaired *t* tests were used to calculate p-values. P < 0.05 was considered a significant difference. (F) Increase of LC3-II in *Atg5*^{flox/flox} but not in *Atg5*^{flox/flox};EL-*Cre2* after cerulein treatment. (G) Serum amylase activity in cerulein-induced acute pancreatitis. Open bars, saline injection (n = 4); black bars, cerulein injection (n = 4). The asterisk indicates the statistical difference between amylase levels in *Atg5*^{flox/flox} and *Atg5*^{flox/flox};EL-*Cre2* mice (*, P < 0.05). Error bars represent SEM. Bars: (A and C) 50 μm; (B and D) 2 μm.

were the same as revealed by Western blot assay (Fig. S3 A). We next examined Ca^{2+} signaling induced by pancreatic exocrine secretagogues CCK octapeptide (CCK8) in fura-2–loaded enzymatically isolated pancreatic acinar cells. Again, *Atg5*-deficient pancreatic acinar cells show similar $[Ca^{2+}]_i$ increases as those of *Atg5*^{flox/flox} mice in response to 100-pM CCK8 stimulation (Fig. S3 B). Both *Atg5*^{flox/flox} and *Atg5*^{flox/flox};EL-*Cre2* mice at 2 mo of age were used in the following experiments.

Figure 5. **Loss of trypsin activation in Atg5-deficient pancreatic acinar cells.** (A and B) Acinar cells derived from Atg5$^{flox/flox}$ and Atg5$^{flox/flox}$;EL-Cre2 mice were incubated with cerulein. Acinar cells were isolated at 2 mo of age by treatment of the pancreas with collagenase. After stimulation with 10 nM cerulein, cells were suspended in the medium with a synthetic trypsin substrate, (CBZ-Ile-Pro-Arg)2-rhodamine 110. Rhodamine fluorescence was detected in 90% of acinar cells of Atg5$^{flox/flox}$ mice but in 33% of acinar cells in Atg5$^{flox/flox}$;EL-Cre2 mice. (C and D) The effects of autophagy and cerulein on the pancreatic trypsin activity (C) and content of TAP (D). Cerulein administration increased the pancreatic trypsin activity and content of TAP in Atg5$^{flox/flox}$ mice but not in Atg5$^{flox/flox}$;EL-Cre2 mice. *, P < 0.01. Error bars represent SEM. Bars, 10 μm.

A

Atg5$^{flox/flox}$ | Atg5$^{flox/flox}$;EL-Cre2

B

| Atg5$^{flox/flox}$ | 190 | 21 | 211 |
| Atg5$^{flox/flox}$;EL-Cre2 | 67 | 135 | 202 |

☐ activated ☐ non-activated

C

Trypsin activity (mU/mg)

D

TAP (ng/mg)

☐ saline ☐ cerulein

Saline injection did not cause any pathological changes in both Atg5$^{flox/flox}$ and Atg5$^{flox/flox}$;EL-Cre2 mice as revealed by histochemical and EM analyses (Fig. 4, A and C). We then induced acute pancreatitis by cerulein in Atg5$^{flox/flox}$ and Atg5$^{flox/flox}$;EL-Cre2 mice. Atg5$^{flox/flox}$ mice showed typical signs of acute pancreatitis, such as severe acinar cell degeneration, edema in connective tissue, and infiltration of inflammatory cells with H&E staining (Fig. 4 B). EM analysis revealed numerous autophagosomes and a decrease of zymogen granules in Atg5$^{flox/flox}$ mice (Fig. 4 B). In contrast, Atg5$^{flox/flox}$;EL-Cre2 mice displayed normal histochemical characteristics except very mild edema in a small restricted region (Fig. 4 D). In fact, autophagosomes were not observed, and zymogen granules appeared to be intact in Atg5$^{flox/flox}$;EL-Cre2 mice (Fig. 4 D). We quantified histological changes using a histological score (Hughes et al., 1996) by a pathologist and showed that there was statistical significant difference in pathological changes by a pathologist between Atg5$^{flox/flox}$ and Atg5$^{flox/flox}$;EL-Cre2 mice (Fig. 4 E). In accordance

with histological and EM examination, LC3-II increased significantly in Atg5$^{flox/flox}$ mice but not in Atg5$^{flox/flox}$;EL-Cre2 mice after cerulein injection (Fig. 4 F). In addition, the serum amylase level in Atg5$^{flox/flox}$;EL-Cre2 mice with cerulein was significantly lower than in Atg5$^{flox/flox}$ mice (Fig. 4 G). There was a slight increase in serum amylase when Atg5$^{flox/flox}$;EL-Cre2 mice were treated with cerulein (Fig. 4 G). This may be caused by stimulation of secretion of digestive enzymes by cerulein itself. Collectively, these results indicate that typical acute pancreatitis is not induced in the absence of autophagy.

The mechanism for much milder acute pancreatitis in the absence of autophagy could be the low level of trypsinogen activation. To test this hypothesis, we analyzed trypsinogen activation by cerulein in primary cultured acinar cells using a highly sensitive method for detection of trypsin activity (Ohmuraya et al., 2006). Trypsinogen activation was observed in 90% (190/211 cells) and 33% (67/202 cells) of acinar cells from Atg5$^{flox/flox}$ and Atg5$^{flox/flox}$;EL-Cre2 mice, respectively (Fig. 5, A and B). We also

used acinar cells isolated from $Atg5$-deficient newborn mice ($Atg5^{-/-}$) in which $Atg5$ was completely inactivated in all cells (Kuma et al., 2004). Trypsinogen activation was observed in 91% (182/201 cells) and 5% (11/217 cells) of acinar cells from $Atg5^{+/-}$ and $Atg5^{-/-}$ mice, respectively. Trypsinogen activation in some acinar cells may be caused by the presence of an alternative pathway for trypsin activation.

We then measured trypsin activity in pancreatic homogenates from $Atg5^{flox/flox}$;EL-$Cre2$ and $Atg5^{flox/flox}$ mice treated with cerulein or saline. In saline controls, there was no difference in the levels of trypsin activities between $Atg5^{flox/flox}$ (0.25 ± 0.09 mU/mg; $n = 3$) and $Atg5^{flox/flox}$;EL-$Cre2$ mice (0.16 ± 0.03 mU/mg; $n = 3$). After cerulein injection, trypsin levels significantly increased in $Atg5^{flox/flox}$ mice (1.97 ± 1.10 mU/mg; $n = 3$) but mildly increased in $Atg5^{flox/flox}$;EL-$Cre2$ mice (0.52 ± 0.41 mU/mg; $n = 3$; Fig. 5 C). Activation of trypsinogen into active trypsin results in the production of trypsinogen activation peptide (TAP), which corresponds to the N-terminal region of the trypsinogen. TAP was quantified in pancreatic homogenates from $Atg5^{flox/flox}$;EL-$Cre2$ and $Atg5^{flox/flox}$ mice treated with cerulein or saline. In saline controls, there was no difference in the levels of TAP between $Atg5^{flox/flox}$ (2.36 ± 0.22 ng/mg; $n = 3$) and $Atg5^{flox/flox}$;EL-$Cre2$ mice (2.08 ± 0.18 ng/mg; $n = 3$). After cerulein injection, TAP levels significantly increased in $Atg5^{flox/flox}$ mice (18.54 ± 2.04; $n = 3$) but not in $Atg5^{flox/flox}$;EL-$Cre2$ mice (5.65 ± 1.19; $n = 3$; Fig. 5 C). All of these data suggest that trypsinogen activation is considerably suppressed by reduced autophagy.

Our findings established that autophagy is induced by supramaximal stimulation of cerulein and is directly related to trypsinogen activation and onset of acute pancreatitis. This is the first example that autophagy plays a destructive role in the early stage of disease development. Although the mechanism for autophagy induction by cerulein is not yet clear, insufficient recruitment of zymogene granule membranes under supramaximal stimulation may account for it. In physiological conditions, digestive enzymes are targeted to the secretory compartment, and mixing of lysosomes with digestive zymogens does not occur in the exocrine pancreas (Gorelick et al., 1992). In autophagy, autophagosomes containing intracellular components fuse with endosomes and lysosomes to form autolysosomes (Dunn, 1990). Thus, trypsinogen could be hydrolyzed to trypsin by a lysosomal enzyme such as cathepsin B in autolysosomes. Thus, we propose the autophagy theory for activation of trypsin in acute pancreatitis, and this can explain both the colocalization hypothesis and autoactivation hypothesis.

Materials and methods

Cerulein-induced pancreatitis
After overnight fasting, mice were given hourly intraperitoneal injections of saline or saline containing 50 μg/kg cerulein (Sigma-Aldrich) for 6, 9, and 12 h. 1 h after the last injection, mice were killed, and serum and pancreas samples were rapidly obtained.

Histological analysis
Tissue was fixed overnight in 10% formalin, embedded in paraffin, sectioned, and stained with H&E. For EM analysis, the pancreas was fixed with 2.5% glutaraldehyde in 0.1 M phosphate buffer, pH 7.4, for 2 h. Conventional EM was performed as previously described (Yamamoto et al., 1991).

Fluorescence microscopic analysis
The pancreas from GFP-LC3 mice was dissected, fixed with 4% PFA, and sectioned, and GFP fluorescence was observed using a fluorescence microscope (IX81; Olympus) equipped with a CCD camera (ORCA ER; Hamamatsu; Mizushima et al., 2004).

Trypsin assay in acinar cells
Isolated acinar cells were cultured with 10 nM cerulein, and trypsin activity was examined by using a synthetic trypsin substrate, (CBZ-Ile-Pro-Arg)2-rhodamine 110 (Invitrogen; Ohmuraya et al., 2006).

Measurement of trypsin activity
Measurement of trypsin activity was performed as described previously (Towatari et al., 2002).

TAP
Pancreas specimens were boiled at 100°C for 15 min in 0.2 M Tris (hydroxymethyl) aminomethane (Tris)-HCl buffer, pH 7.3, containing 20 mM EDTA. Samples were homogenized on ice for 30 s and centrifuged at 1,500 g for 10 min at 4°C. TAP was quantified in an aliquot of each supernatant using an enzyme immunoassay kit (Oriental Yeast Co.). The total protein concentration was determined, and pancreatic tissue TAP levels were expressed as nanograms/milligrams of total protein.

Western blot analysis
Conventional Western blot analysis was performed as previously described (Ohmuraya et al., 2005). Rabbit anti-LC3 antibody (MBL International), goat antiamylase antibody (Santa Cruz Biotechnology, Inc.), rabbit antitrypsinogen antibody (Nordic Immunological Laboratories), and rabbit anti-IP3R1-3 antibody (Chemicon) were used at 1:2,000, 1:1,000, 1:1,000, and 1:2,000 dilutions, respectively.

Generation of pancreatic acinar cell–specific Cre recombinase expression mice
pNintCre contained five fragments: NLS derived from SV40, splice donor and intron derived from rabbit β globin, intron and splice acceptor derived from mouse En2, the cre recombinase gene, and the polyadenylation signal derived from SV40. The elastase I gene is selectively expressed in pancreatic acinar cells (Hammer et al., 1987). The DNA fragment containing EL was obtained by PCR using the primers 5'-TGGTGGGAGACATTCCAACAACA-3' for s1 and 5'-TGTGGAGAGATAGACCACTGCC-3' for a2. A fragment containing EL was digested and inserted into pNintCre to generate pEL-Cre (Fig. 3 A). Fragments excised from the pEL-Cre plasmid were separated and used for microinjection. Transgenic founder mice (EL-Cre) were backcrossed with C57BL/6J mice.

RNA analysis
Total RNA was isolated from each organ at 2 mo after birth with Sepasol (Nacalai Tesque). RT-PCR analysis was performed using the primers 5'-AATGCTTCTGTCCGTTTGCC-3' and 5'-GATTTCCGTCTCTGGTGTAG-3' for cre recombinase (563 bp) and 5'-GGAAAGCTGTGGCGTGATG-3' and 5'-CTGTTGCTGTAGCCGTATTC-3' for G3PDH (382 bp).

Generation of pancreatic acinar cell–specific Atg5-deficient mice
Mice bearing an $Atg5$ flox allele ($Atg5^{flox}$) were crossed with a transgenic line, EL-Cre2. These mice caused deletion of the loxP-flanked exon 3 of the $Atg5$ gene. The deleted allele was detected by PCR with the primers 5'-CAGGGAATGGTGTCTCCCAC-3' for D (5L2) and 5'-GTACTGCATAATG-GTTTAACTCTTGC-3' for B (short2). Southern blot analysis was performed as previously described (Hara et al., 2006).

Measurement of [Ca²⁺]i
CCK-8 was obtained from the Peptide Institute, and Fura-2AM was obtained from Dojindo. Measurement of intracellular Ca²⁺ concentration in pancreatic acinar cell suspensions was performed as previously described (Futatsugi et al., 2005) using an Aquacosmos ratio (Hamamatsu).

Online supplemental material
Fig. S1 shows the pancreas of $Atg5^{flox/flox}$ and $Atg5^{flox/flox}$;EL-Cre2 mice. Fig. S2 shows Western blot analysis using antiamylase and antitrypsinogen antibodies at embryonic day 18.5, at 0.5 d after birth, and at 2 mo. Fig. S3 shows Western blot analysis of IP3R subtypes in the pancreas and [Ca²⁺]i changes induced by CCK8 receptor stimulation in pancreatic cells. Online supplemental material is available at http://www.jcb.org/cgi/content/full/jcb.200712156/DC1.

References

Adler, G., C. Hahn, H.F. Kern, and K.N. Rao. 1985. Cerulein-induced pancreatitis in rats: increased lysosomal enzyme activity and autophagocytosis. *Digestion.* 32:10–18.

Cuervo, A.M. 2004. Autophagy: in sickness and in health. *Trends Cell Biol.* 14:70–77.

Dunn, W.A. Jr. 1990. Studies on the mechanisms of autophagy: maturation of the autophagic vacuole. *J. Cell Biol.* 110:1935–1945.

Futatsugi, A., T. Nakamura, M.K. Yamada, E. Ebisui, K. Nakamura, K. Uchida, T. Kitaguchi, H. Takahashi-Iwanaga, T. Noda, J. Aruga, and K. Mikoshiba. 2005. IP3 receptor types 2 and 3 mediate exocrine secretion underlying energy metabolism. *Science.* 309:2232–2234.

Gorelick, F.S., I.M. Modlin, S.D. Leach, R. Carangelo, and M. Katz. 1992. Intracellular proteolysis of pancreatic zymogens. *Yale J. Biol. Med.* 65:407–420 (discussion 437–440).

Hammer, R.E., G.H. Swift, D.M. Ornitz, C.J. Quaife, R.D. Palmiter, R.L. Brinster, and R.J. MacDonald. 1987. The rat elastase I regulatory element is an enhancer that directs correct cell specificity and developmental onset of expression in transgenic mice. *Mol. Cell. Biol.* 7:2956–2967.

Hara, T., K. Nakamura, M. Matsui, A. Yamamoto, Y. Nakahara, R. Suzuki-Migishima, M. Yokoyama, K. Mishima, I. Saito, H. Okano, and N. Mizushima. 2006. Suppression of basal autophagy in neural cells causes neurodegenerative disease in mice. *Nature.* 441:885–889.

Helin, H., M. Mero, H. Markkula, and M. Helin. 1980. Pancreatic acinar ultrastructure in human acute pancreatitis. *Virchows Arch. A Pathol. Anat. Histol.* 387:259–270.

Hirota, M., M. Ohmuraya, and H. Baba. 2006. Genetic background of pancreatitis. *Postgrad. Med. J.* 82:775–778.

Hughes, C.B., A.B. el-Din, M. Koth, L.W. Gaber, and A.O. Gaber. 1996. Calcium channel blockade inhibits release of TNF alpha and improves survival in a rat model of acute pancreatitis. *Pancreas.* 13:22–28.

Ichimura, Y., T. Kirisako, T. Takao, Y. Satomi, Y. Shimonishi, N. Ishihara, N. Mizushima, I. Tanida, E. Kominami, M. Ohsumi, et al. 2000. A ubiquitin-like system mediates protein lipidation. *Nature.* 408:488–492.

Kabeya, Y., N. Mizushima, T. Ueno, A. Yamamoto, T. Kirisako, T. Noda, E. Kominami, Y. Ohsumi, and T. Yoshimori. 2000. LC3, a mammalian homologue of yeast Apg8p, is localized in autophagosome membranes after processing. *EMBO J.* 19:5720–5728.

Klionsky, D.J. 2005. The molecular machinery of autophagy: unanswered questions. *J. Cell Sci.* 118:7–18.

Klionsky, D.J., J.M. Cregg, W.A. Dunn, S.D. Emr, Y. Sakai, I.V. Sandoval, A. Sibirny, S. Subramani, M. Thumm, M. Veenhuis, and Y. Ohsumi. 2003. A unified nomenclature for yeast autophagy-related genes. *Dev. Cell.* 5:539–545.

Koike, H., M.L. Steer, and J. Meldolesi. 1982. Pancreatic effects of ethionine: blockade of exocytosis and appearance of crinophagy and autophagy precede cellular necrosis. *Am. J. Physiol.* 242:G297–G307.

Komatsu, M., S. Waguri, T. Ueno, J. Iwata, S. Murata, I. Tanida, J. Ezaki, N. Mizushima, Y. Ohsumi, Y. Uchiyama, et al. 2005. Impairment of starvation-induced and constitutive autophagy in Atg7-deficient mice. *J. Cell Biol.* 169:425–434.

Kuma, A., M. Hatano, M. Matsui, A. Yamamoto, H. Nakaya, T. Yoshimori, Y. Ohsumi, T. Tokuhisa, and N. Mizushima. 2004. The role of autophagy during the early neonatal starvation period. *Nature.* 432:1032–1036.

Leach, S.D., I.M. Modlin, G.A. Scheele, and F.S. Gorelick. 1991. Intracellular activation of digestive zymogens in rat pancreatic acini. Stimulation by high doses of cholecystokinin. *J. Clin. Invest.* 87:362–366.

Mizushima, N. 2005. The pleiotropic role of autophagy: from protein metabolism to bactericide. *Cell Death Differ.* 12:1535–1541.

Mizushima, N., A. Yamamoto, M. Matsui, T. Yoshimori, and Y. Ohsumi. 2004. In vivo analysis of autophagy in response to nutrient starvation using transgenic mice expressing a fluorescent autophagosome marker. *Mol. Biol. Cell.* 15:1101–1111.

Ohmuraya, M., M. Hirota, M. Araki, N. Mizushima, M. Matsui, T. Mizumoto, K. Haruna, S. Kume, M. Takeya, M. Ogawa, et al. 2005. Autophagic cell death of pancreatic acinar cells in serine protease inhibitor Kazal type 3-deficient mice. *Gastroenterology.* 129:696–705.

Ohmuraya, M., M. Hirota, K. Araki, H. Baba, and K. Yamamura. 2006. Enhanced trypsin activity in pancreatic acinar cells deficient for serine protease inhibitor kazal type 3. *Pancreas.* 33:104–106.

Sherwood, M.W., I.A. Prior, S.G. Voronina, S.L. Barrow, J.D. Woodsmith, O.V. Gerasimenko, O.H. Petersen, and A.V. Tepikin. 2007. Activation of trypsinogen in large endocytic vacuoles of pancreatic acinar cells. *Proc. Natl. Acad. Sci. USA.* 104:5674–5679.

Soriano, P. 1999. Generalized lacZ expression with the ROSA26 Cre reporter strain. *Nat. Genet.* 21:70–71.

Steer, M.L., and J. Meldolesi. 1987. The cell biology of experimental pancreatitis. *N. Engl. J. Med.* 316:144–150.

Towatari, T., M. Ide, K. Ohba, Y. Chiba, M. Murakami, M. Shiota, M. Kawachi, H. Yamada, and H. Kido. 2002. Identification of ectopic anionic trypsin I in rat lungs potentiating pneumotropic virus infectivity and increased enzyme level after virus infection. *Eur. J. Biochem.* 269:2613–2621.

Tsukada, M., and Y. Ohsumi. 1993. Isolation and characterization of autophagy-defective mutants of *Saccharomyces cerevisiae*. *FEBS Lett.* 333:169–174.

van Acker, G.J., G. Perides, and M.L. Steer. 2006. Co-localization hypothesis: a mechanism for the intrapancreatic activation of digestive enzymes during the early phases of acute pancreatitis. *World J. Gastroenterol.* 12:1985–1990.

Watanabe, O., F.M. Baccino, M.L. Steer, and J. Meldolesi. 1984. Supramaximal caerulein stimulation and ultrastructure of rat pancreatic acinar cell: early morphological changes during development of experimental pancreatitis. *Am. J. Physiol.* 246:G457–G467.

Yamamoto, A., H. Otsu, T. Yoshimori, N. Maeda, K. Mikoshiba, and Y. Tashiro. 1991. Stacks of flattened smooth endoplasmic reticulum highly enriched in inositol 1,4,5-trisphosphate (InsP3) receptor in mouse cerebellar Purkinje cells. *Cell Struct. Funct.* 16:419–432.

In This Issue
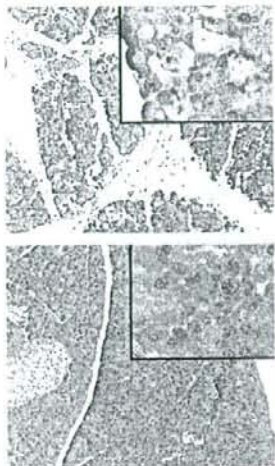
Cellular self-eating promotes pancreatitis

To survive tough times, cells sometimes resort to a form of self-cannibalism called autophagy. But as Hashimoto et al. reveal, autophagy can have a down side, destroying the pancreas by prematurely activating a digestive enzyme.

In autophagy, a vesicle swallows a portion of cytoplasm and ferries it to the lysosome for digestion. The process is often beneficial, allowing hungry cells to recycle molecules, for example. However, the researchers previously discovered that in mice with pancreatitis the level of autophagy in pancreatic cells surges. Pancreatitis occurs when the enzyme trypsin dissolves cells from within. Normally, pancreatic cells fashion and discharge an inactive form of trypsin called trypsinogen, which remains inert until it reaches the small intestine. But if trypsinogen converts to trypsin before its release, it can damage or kill a pancreatic cell. Hashimoto et al. tested whether autophagy promotes this early activation by delivering trypsinogen to the lysosome, where enzymes turn it on.

The researchers gave mice injections of the compound cerulein, which spurs pancreatitis. Control animals suffered severe damage to the organ, which harbored numerous deteriorating cells. But rodents that lack a gene necessary for autophagy displayed almost no symptoms. To determine whether autophagy promotes trypsinogen activation, the team dosed pancreatic cells from both types of mice with cerulein. Cells from the autophagy-impaired animals carried much less activated trypsinogen than did cells from controls.

In rodents capable of autophagy, cerulein injections triggered much higher levels of trypsin activity in pancreatic tissue than did shots of saline, confirming that autophagy switches on the enzyme. The study is the first to reveal that autophagy can initiate a disease. The next step, the researchers say, is determining what triggers pancreatic cells to start eating themselves. JCB

Hashimoto, D., et al. 2008. *J. Cell Biol.* doi:10.1083/jcb.200712156.

Pancreatic tissue from a control mouse shows damage from pancreatitis (top), but tissue from a mouse that can't instigate autophagy is healthy (bottom).

Alzheimer's protein controls calcium's ins and outs

Two enzymes that help manufacture amyloid β, the protein that accumulates in the brain in Alzheimer's disease, also take on another job. As Green et al. report, the enzymes, known as presenilins, help set calcium levels inside cells by activating a pump protein.
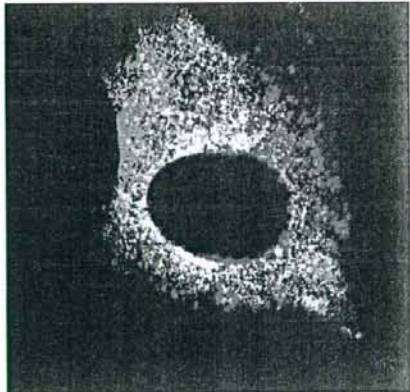
Presenilins partner with other proteins to create the enzyme γ-secretase, which helps snip amyloid β into shape. Faulty presenilins trigger a rare, early-onset variant of Alzheimer's disease (AD) that strikes patients who are under 65 yr old. Presenilins might also help dictate how much calcium enters and exits the ER, which serves as the cell's storehouse for the ion. For instance, ER calcium release skyrockets in cells from patients with early onset AD. And in cells lacking one of the presenilins, the ER contains less calcium than normal. These results suggest that the presenilins help regulate SERCA, the protein that pumps calcium into storage.

To test that possibility, Green et al. eliminated both presenilins from cells and found that their cytoplasmic calcium levels were higher than normal. The scientists also measured how rapidly frog eggs shuttled a controlled influx of calcium ions into the ER. Engineering the eggs to manufacture presenilins, which they don't normally make, accelerated calcium pumping into the ER.

The location of presenilins and SERCA reflects their close relationship, the team found. Presenilins not only settle alongside SERCA in the ER, they attach to the pump protein. Green et al. also discovered a link between amyloid β and SERCA: increased SERCA activity translated into higher amyloid β production. SERCA might exert this effect by prodding γ-secretase, the team concludes.

The results show that along with forming part of the protein-slicing γ-secretase complex, presenilins are crucial for regulating intracellular calcium homeostasis. Both functions allow the enzymes to exert control over amyloid β formation. JCB

Green, K.N., et al. 2008. *J. Cell Biol.* doi:10.1083/jcb.200706171.

Presenilin (red) and SERCA (green) cozy up in this fibroblast.

Text by Mitch Leslie

mitchleslie@comcast.net

How cells make local calls

Broadcast a message over a loudspeaker, and you can't be sure who will hear it. But whisper the message into the friend's ear, and you can be sure it got through. Cells follow a similar strategy when they transmit signals with reactive oxygen species (ROS), as Chen et al. show. By positioning the sender and recipient molecules near each other, cells ensure efficient communication.

ROS are best known as destructive byproducts of metabolism that might cause aging. But cells also use the molecules to carry messages. The mystery is how cells direct ROS to their targets, since some ROS can diffuse throughout the cell, potentially reacting with any molecules they encounter.

Proximity is the key, Chen et al. found. They tracked down the signal-relaying molecule NADPH oxidase 4 (Nox4), which produces the ROS hydrogen peroxide. The protein was stationed in the endoplasmic reticulum near another protein called PTP1B, which slows division of endothelial cells by turning down the epidermal growth factor receptor (EGFR). The team showed that Nox4 was oxidizing and shutting down adjacent PTP1B molecules. Using an antioxidant that homes in on the ER, for instance, the team could block EGFR signaling, indicating that oxidation of PTP1B had been prevented. An antioxidant that remains in the cytoplasm, however, had no effect on the receptor. The results suggest that by keeping Nox4 and PTP1B close together in the ER, cells make it easier for ROS signals to travel between them. One question the researchers now want to answer is what activates Nox4 in the first place. JCB

Chen, K., et al. 2008. *J. Cell Biol.* doi:10.1083/jcb.200709049.

Golgi-derived vesicles (green) amass at the cleavage furrow.

Daughter cells share duties

There's no sibling rivalry during cell division. Goss and Toomre show that during cytokinesis both daughter cells pitch in to supply new membrane.

Researchers suspect that during cytokinesis, fresh membrane shuttles to the junction between the two daughter cells. Where the membrane comes from has puzzled researchers. A previous study using spinning disc confocal microscopy suggested that only one daughter cell provides it. However, that study didn't track individual membrane vesicles.

Goss and Toomre were able to do just that by capturing images 60 times faster. They found that vesicles from both daughter cells leave the Golgi apparatus and cruise to the cleavage furrow, accumulating there. Although other potential sources of membrane, including endosomes, also collect near the furrow, they remain aloof from the Golgi-derived vesicles that will ultimately fuse with the cell membrane.

With total internal reflection fluorescence microscopy, the team observed individual vesicles from both daughter cells merging with the plasma membrane at the cleavage furrow. However, the results don't necessarily conflict with the previous study, the researchers say. They note that they also observed an asymmetric stage in which only one cell appears to direct vesicles to the cleavage furrow. JCB

Goss, J.W., and D.K. Toomre. 2008. *J. Cell Biol.* doi:10.1083/jcb.200712137.

In fused cells, there's little mixing between the two kinds of mitochondrial DNA (red and green).
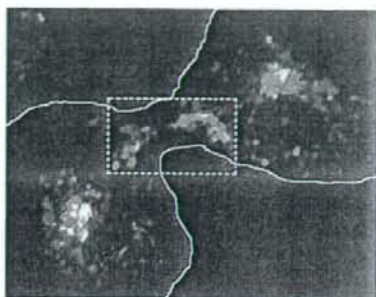
Mitochondrial DNA stays home

Mitochondria stow their DNA in structures called nucleoids. As Gilkerson et al. reveal, nucleoids are selfish and don't share their DNA with each other. The results might help explain some quirks of mitochondrial inheritance and support a proposed treatment strategy for illnesses caused by defects in the organelles.

A nucleoid can house up to 10 copies of a mitochondrion's genome. One reason that the structures intrigue researchers is that they might help control how the DNAs get parceled out when mitochondria divide. To understand mitochondrial DNA inheritance, researchers need to resolve whether nucleoids swap DNA. The question has remained unanswered because of the difficulty of tracking individual mitochondrial DNAs.

To overcome that problem, Gilkerson et al. fused two kinds of cells, each of which carried a different mitochondrial genome. In the merged cells, the researchers found, labeled versions of the two types of mitochondrial DNA rarely appeared together, suggesting that the nucleoids weren't mingling their contents. Stingy nucleoids could explain why cells that harbor a variety of mitochondrial genomes sometimes lose DNA diversity as they divide and sometimes don't. The outcome might depend on whether the DNAs in a particular nucleoid are uniform or varied. The results also offer support for plans to treat mitochondrial diseases by nudging cells to eliminate defective DNA. The lack of swapping will make it easier to purge faulty mitochondrial genomes, the researchers say. JCB

Gilkerson, R.W., et al. 2008. *J. Cell Biol.* doi:10.1083/jcb.200712101.

How I Do It

Percutaneous transfistulous pancreatic duct drainage and interventional pancreatojejunostomy as a treatment option for intractable pancreatic fistula

Masahiko Hirota, M.D.[a],*, Keiichiro Kanemitsu, M.D.[b], Hiroshi Takamori, M.D.[b],
Akira Chikamoto, M.D.[b], Naoko Hayashi, M.D.[b], Kei Horino, M.D.[b],
Hideo Baba, M.D.[b]

[a]*Department of Surgery, Kumamoto Regional Medical Center, Kumamoto-city, Japan;* [b]*Department of Gastroenterological
Surgery, Kumamoto University Graduate School of Medical Sciences, Kumamoto-city, Japan*

KEYWORDS:
Pancreatic fistula;
Pancreatojejunostomy;
Pancreatoduodenectomy;
Distal pancreatectomy

Abstract. We present 2 techniques for treatment of intractable pancreatic fistula: percutaneous trans-fistulous pancreatic duct drainage and interventional pancreatojejunostomy. Percutaneous transfistulous pancreatic duct drainage can be effective for intractable fistulas that communicate with the main pancreatic duct. Because drainage itself is not enough for a complete cure of this complication when it occurs in cases after pancreatoduodenectomy (PD), interventional pancreatojejunostomy is applicable.
© 2008 Published by Elsevier Inc.

Pancreatic fistula remains a significant problem in pancreatobiliary surgery. Pancreatic resection, including pancreatoduodenectomy (PD) and distal pancreatectomy (DP), has become an increasingly common and safe operation for selected patients with pancreatic and/or extrahepatic biliary disorders. Despite decreased morbidity and mortality rates after pancreatic resection, pancreatic fistula remains a common and potentially lethal complication after pancreatectomy. Its reported incidence varies from 6% to 38%.[1–7] Eighty-five percent to 95% of pancreatic fistula cases can be managed using a combination of external drainage and medical therapy.[3,8] However, occasional patients with inadequately drained intra-abdominal inflammation may require re-operation. When it occurs, prompt recognition and proper management of pancreatic fistula are important.

If pancreatic fistula occurs, the pancreatic juice must be drained externally to avoid intra-abdominal hemorrhage and sepsis. We have devised and successfully performed percutaneous transfistulous canulation and drainage of the main pancreatic duct (percutaneous pancreatic duct drainage) for 2 pancreatic fistula cases. Furthermore, in the case of pancreatic fistula after PD, interventional pancreatojejunostomy was also performed successfully.

Techniques

Percutaneous pancreatic duct drainage

This technique is useful for major pancreatic fistula in which the main pancreatic duct is visualized in fistulography. Any abscess due to pancreatic fistula is first drained percutaneously. Using the abscess drainage tube as a sheath, an angled angiography catheter (RIM catheter or RC2 catheter, Medikit, Tokyo, Japan) is inserted into the main pancreatic duct via the abscess and fistula (Fig. 1). Using this type of catheter, the tip is straight when placed within the sheath, and curves if it

* Corresponding author. Tel.: +81-96-363-3311; fax: +81-96-362-0222.
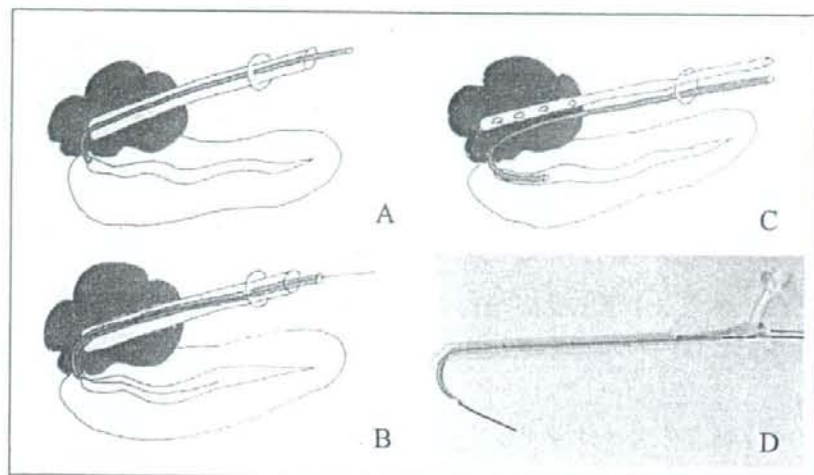E-mail address: mhirota@krmc.or.jp

Figure 1   Percutaneous pancreatic duct drainage. Using the abscess drainage tube as a sheath, an angled catheter is inserted into the main pancreatic duct via the abscess and fistula (A, B, C). The abscess is drained using another catheter (C). (D) RC2 angled angiography catheter.

protrudes from the sheath. By twisting and taking the catheter in and out of the sheath, the route into the pancreatic duct can be selected. After placing the catheter into the main pancreatic duct, the abscess is drained using another catheter (Fig. 1C). Because almost all pancreatic juice drained externally with this system, the abscess is cured within a short period.

Interventional pancreatojejunostomy

A guidewire is inserted into the jejunum using an intrajejunally placed tube. The guidewire, grasped by a basket catheter inserted from the percutaneous transhepatic biliary drainage (PTBD) route under fluoroscopy, is led externally via the PTBD outlet (Fig. 2A and B). A drainage catheter is inversely inserted into the remnant pancreatic duct over the guidewire via the PTBD route and the jejunum (Fig. 2C and D). We control the position of the drainage catheter by pulling a thread placed on its tip (Fig. 2C and D). Pancreatic juice then flows along the drainage catheter from the pancreas to outside of the body via the jejunum and intrahepatic bile duct. After 1 month, the drainage catheter is removed.
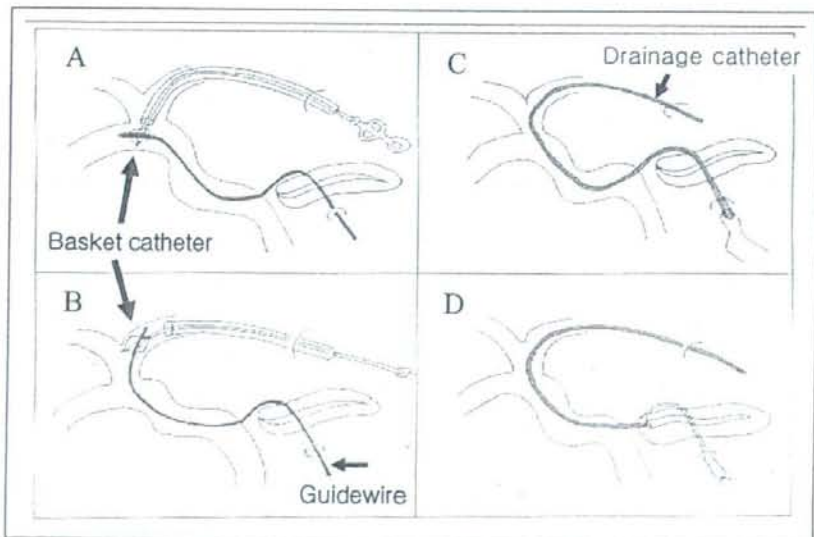

Figure 2   Interventional pancreatojejunostomy. A guidewire in the jejunum is grasped and led externally by a basket catheter inserted from PTBD route (A, B). A drainage catheter is inversely inserted into the remnant pancreatic duct over the guidewire (C, D).
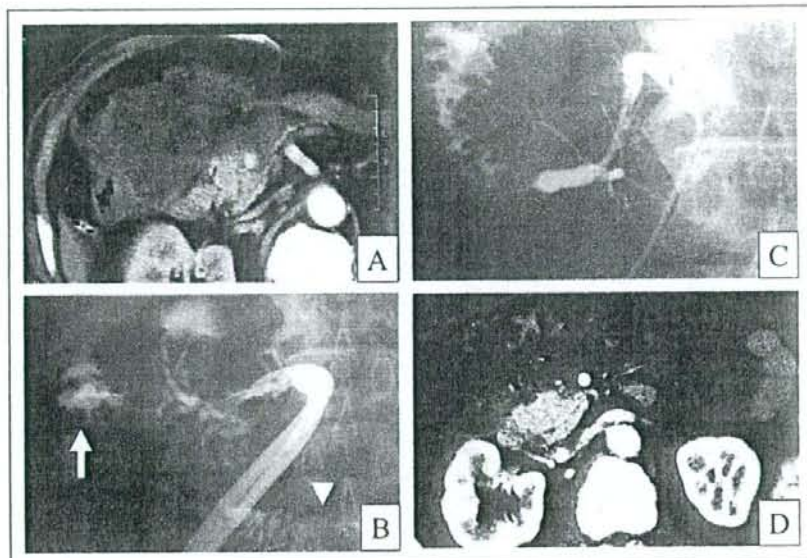
Figure 3 Percutaneous pancreatic duct drainage in case 1. A huge abscess was formed in the right upper quadrant (A). It was found to have penetrated into the transverse colon (arrow) and duodenum (arrowhead) (B). A drainage catheter was inserted into the main pancreatic duct (C). (D) CT scan 1 month after percutaneous pancreatic duct drainage.

Case Presentation

Case 1

A 56-year-old man presented with severe sepsis due to a pancreatic fistula after DP. On computed tomography (CT) scan, a huge abscess was found in the right upper quadrant (Fig. 3A). After percutaneous drainage, the abscess was found to have penetrated into the transverse colon and duodenum (Fig. 3B). Because the main pancreatic duct was present in the remnant pancreas head, the drainage catheter was inserted into the main pancreatic duct to drain the pancreatic juice directly (Fig. 3C). CT scan 1 month later showed complete disappearance of the abscess (Fig. 3D).

Case 2

A 78-year-old man presented with severe sepsis due to a pancreatic fistula after PD. An abscess had formed around the pancreatojejunal anastomosis (Fig. 4A). As in case 1, we drained the abscess percutaneously and then inserted a drainage catheter into the main pancreatic duct of the remnant pancreatic body and tail via the pancreatic fistula (Fig. 4B). A drainage catheter was also inserted into the jejunum via the fistula route (Fig. 4C). Draining the main pancreatic duct cured the abscess. However, because simple drainage was not sufficient to cure the pancreatic fistula after PD, we then performed interventional pancreatojejunostomy. A guidewire was grasped

using a basket catheter and then led outside the body via the PTBD outlet (Fig. 5A, B). A drainage catheter was inserted into the remnant pancreatic duct via the PTBD route and jejunum (Fig. 5C and D). Figure 5 corresponds to each procedure in Fig. 2. Magnetic resonance cholangiopancreatography 6 months later showed an uninterrupted pancreatic duct connected with the jejunum without any leakage (Fig. 4D).

Comments

Pancreatic fistulas represent the most common and clinically relevant of surgical complications, with consequences that are life-threatening (ie, bleeding, sepsis). We presented 2 techniques, percutaneous transfistulous pancreatic duct drainage and interventional pancreatojejunostomy, as treatment options for intractable pancreatic fistula. Since visualization of the main pancreatic duct indicates that the pancreatic fistula is intractable. Fistulography (used in these cases) may help visualize communication with the main pancreatic duct.

In a prospective study in which CT was used routinely, postoperative acute pancreatitis, which was diagnosed in 26% of patients who had undergone pancreatic resection, was strongly associated with other postoperative complications, including pancreatic fistula.[9] In cases with DP, an inability to find the main pancreatic duct for ligation was a major factor of postoperative fistula in cases with DP.[10,11] Pancreatic fistula also occurs in acute or chronic pancreati-
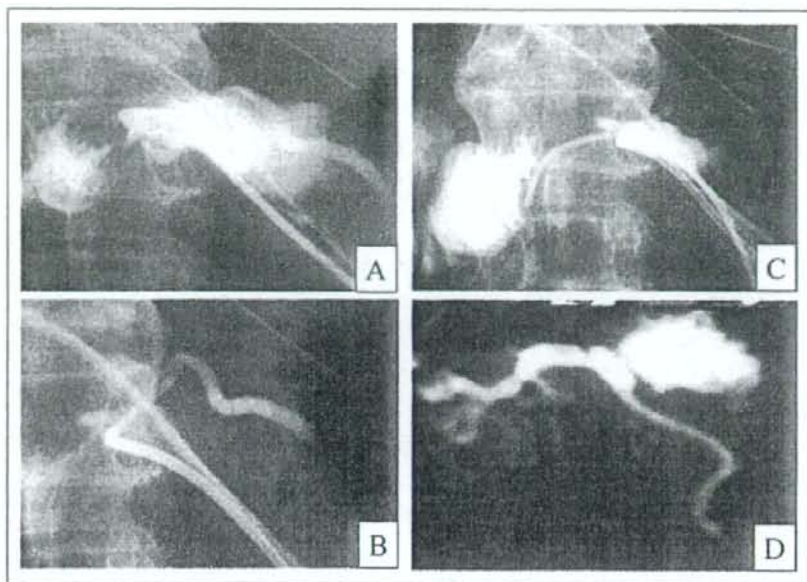
Figure 4   Percutaneous pancreatic duct drainage in case 2. An abscess around the pancreatojejunostomy was drained percutaneously (A). Drainage catheters were inserted into the pancreatic duct (B) and jejunum (C). (D) MRCP after completion of interventional pancreatojejunostomy.

tis. Disruption of the main pancreatic duct from an acute or chronic inflammatory process can result in an internal pancreatic fistula.

The conventional treatment strategy for postoperative pancreatic fistula consists of establishing adequate external drainage and fistula control, treating infection, providing
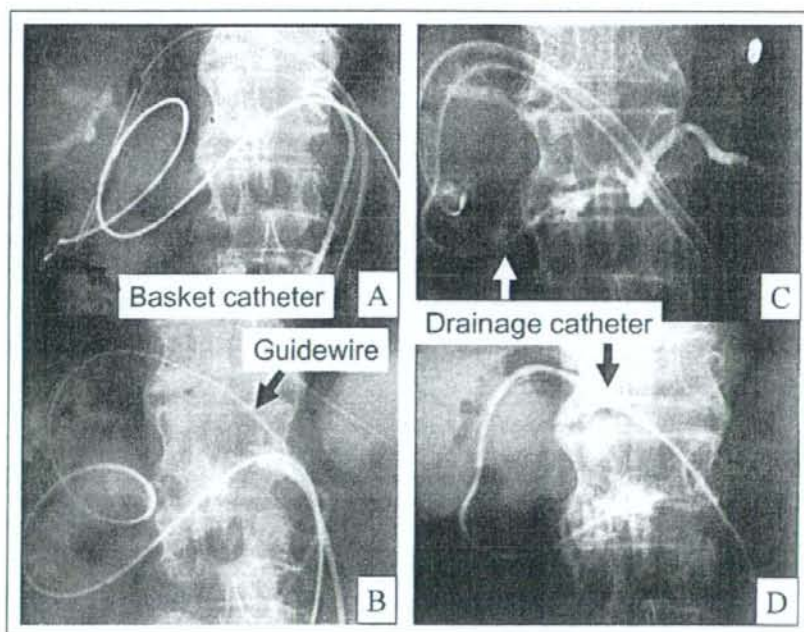

Figure 5   Interventional pancreatojejunostomy in case 2. A guidewire was grasped and led externally by a basket catheter inserted from PTBD route (A, B). A drainage catheter was successfully inserted into the remnant pancreatic duct via PTBD route and jejunum (C, D).

nutritional support, and reducing pancreatic juice secretion by total parenteral nutrition or octreotide. With effective drainage, most of the pancreatic fistula can be cured by conservative treatment. However, the management of intractable pancreatic fistula cases has not been standardized and remains challenging. The management of intractable pancreatic fistula must be individualized. Several devices have been reported, including occlusion of the pancreatic duct by tissue glues such as prolamine,[12–14] ethylene-vinyl alcohol[15] and fibrin glue,[16] endoscopic drainage,[17,18] percutaneous intervention,[14,19] and surgical treatment such as completion pancreatectomy.[20] The vast majority of pancreatic fistulas, which are characterized by maintained continuity with an unobstructed main pancreatic duct (side fistula), respond well to conservative treatment.[21] However, pancreatic fistulas that lose continuity with the left side of the main pancreatic duct and gastrointestinal tract (end fistula, as in case 2) or with the downstream duct obstruction due to stricture, stone, or neoplasm do not respond to conservative treatment.

Transpapillary stents can bypass the high resistance of the sphincter of Oddi, ductal strictures, and calculi, thereby reducing the intraductal pressure that is the driving force behind the fistula. Endoscopic pancreatic sphincterotomy is also recommended for the treatment of pancreatic fistula after DP.[14] However, the communication routes between the duodenum and pancreatic duct that are created by these procedures may sometimes exaggerate infection. From this standpoint, percutaneous transfistulous drainage, if possible, is preferable.

References

1. Schmidt CM, Powell ES, Yiannoutsos CT, et al. Pancreaticoduodenectomy: a 20-year experience in 516 patients. Arch Surg 2004;139:718–27.
2. Okabayashi T, Kobayashi M, Sugimoto T, et al. Postoperative pancreatic fistula following surgery for gastric and pancreatic neoplasm; is distal pancreaticosplenectomy truly safe? Hepatogastroenterology 2005;52:233–6.
3. Kazanjian KK, Hines OJ, Eible G, et al. Management of pancreatic fistulas after pancreaticoduodenectomy. Arch Surg 2005;140:849–55.
4. Fischer CP, Hong JC. Early perioperative outcomes and pancreaticoduodenectomy in a general surgery residency training program. J Gastrointest Surg 2006;10:478–82.
5. Nakao A, Fujii T, Sugimoto H, et al. Is pancreaticogastrostomy safer than pancreaticojejunostomy? J Hepatobiliary Pancreat Surg 2006;13:202–6.
6. Muscari F, Suc B, Kirzin S, et al. Risk factors for mortality and intra-abdominal complications after pancreatoduodenectomy: multivariate analysis in 300 patients. Surgery 2006;139:591–8.
7. Balzano G. Zerbi A, Cristallo M, et al. The unsolved problem of fistula after left pancreatectomy: the benefit of cautious drain management. J Gastrointest Surg 2005;9:837–42.
8. Munoz-Bongrand N, Sauvanet A, Denys A, et al. Conservative management of pancreatic fistula after pancreaticoduodenectomy with pancreaticogastrostomy. J Am Coll Surg 2004;199:198–203.
9. Raty S, Sand J, Lantto E, et al. Post-operative acute pancreatitis as a major determinant of post-operative delayed gastric emptying after pancreaticoduodenostomy. J Gastrointest Surg 2006;10:1131–9.
10. Pannegeon V, Pessaux P, Sauvanet A, et al. Pancreatic fistula after distal pancreatectomy. Arch Surg 2006;141:1071–6.
11. Howard TJ, Stonerock CE, Sarkar J, et al. Contemporary treatment strategies for external pancreatic fistulas. Surgery 1998;124:627–33.
12. Hirota M, Kamekawa K, Tashima T, et al. Percutaneous embolization of the distal pancreatic duct to treat intractable pancreatic juice fistula. Pancreas 2001;22:214–6.
13. Bonatti H, Taberalli W, Berger N, et al. Successful management of a proximal pancreatic duct fistula following pancreatic transplantation. Dig Dis Sci 2006;51:2026–30.
14. Casadei R, Bassi F, Calculli L, et al. Report of three cases of chronic pancreatic fistulas treated with prolamine as a sclerosing substance following pancreatic resection. J Pancreas 2006;7:41–6.
15. Zuber-Jerger I, Herold T, Kullmann F. Transpapillary sealing of a pancreatic fistula with Onyx. Gastrointest Endosc 2006;63:1068–9.
16. Haber GB. Tissue glue for pancreatic fistula. Gastrointest Endosc 2004;59:122–5.
17. Cohen SA, Siegel JH. Endotherapy for pancreatic fistulae: inside out or outside in? Am J Gastroenterol 2007;102:525–6.
18. Halttumen J, Weckman L, Kemppainen E, et al. The endoscopic management of pancreatic fistulas. Surg Endosc 2005;19:559–62.
19. Cho A, Arita S, Koike N, et al. Two-staged hepato-pancreatoduodenectomy and interventional pancreaticojejunostomy. Hepatogastroenterology 2005;52:2886–8.
20. Alexakis N, Sutton R, Neoptolemos JP. Surgical treatment of pancreatic fistula. Dig Surg 2004;21:262–74.
21. Howard T, Stonerock C, Sarkar J, et al. Contemporary treatment strategies for external pancreatic fistula. Surgery 1998;124:627–33.

Oxysterol binding protein-related protein-5 is related to invasion and poor prognosis in pancreatic cancer

Yoshikatsu Koga,[1] Shinji Ishikawa,[1] Tadahiko Nakamura,[1] Toshiro Masuda,[1] Yohei Nagai,[1] Hiroshi Takamori,[1] Masahiko Hirota,[1] Keiichiro Kanemitsu,[1] Yoshifumi Baba[1,2] and Hideo Baba[1,3]

[1]Department of Gastroenterological Surgery, Graduate School of Medical Sciences, Kumamoto University; [2]Department of Surgical Pathology, Kumamoto University Hospital, 1-1-1 Honjo, Kumamoto 860-8556, Japan

In previous studies, the gene expression profiles of two hamster pancreatic cancer cells with different potentials for invasion and metastasis were analyzed. In the present study, we identified that one of the genes expressed strongly in the highly metastatic cell line is hamster oxysterol binding protein-related protein (ORP)-5. The aim of the present study was to clarify the relationship between ORP5 and invasion and poor prognosis of human pancreatic cancer. Invasion assays were carried out in both hamster and human pancreatic cancer cells by suppressing the *ORP5* gene with short interfering RNA or inducing its expression by introducing an expression vector. To evaluate the relationship between ORP5 and the characteristics of human pancreatic cancer, 56 pancreatic cancer tissue specimens were analyzed and the ORP5 expression in each pancreatic cancer tissue specimen was analyzed by immunohistochemistry. In both the hamster and human pancreatic cancer cells, suppression of ORP5 significantly reduced the invasion rate of the cells and induction of ORP5 significantly enhanced the invasion rate of the cells. In the clinical sample, the median survival times of the patients with ORP5-positive ($n = 33$) and ORP5-negative ($n = 23$) cancer were 8.3 and 17.2 months, respectively ($P = 0.02$). Also, the 1-year survival rates of patients with ORP5-positive and ORP5-negative cancer were 36.4 and 73.9%, respectively ($P = 0.005$). The ORP5 expression level was related to both invasion and poor prognosis in human pancreatic cancer. These findings suggest that the expression of ORP5 may induce cancer cell invasion, resulting in the poor prognosis of pancreatic cancer. (*Cancer Sci* 2008; 99: 2387–2394)

P ancreatic cancer is one of the most malignant tumors. In most cases, patients are already at an advanced stage of the disease at the time of diagnosis. The main reason for the poor prognosis is not only that these cancers are difficult to detect by ultrasonography or computed tomography, but also that they exhibit great potential for invasion and metastasis. To establish an effective treatment strategy for pancreatic cancer, it is necessary to clarify the cellular and molecular mechanisms of invasion and metastasis in pancreatic cancer.

In our previous studies, we established two hamster pancreatic cancer cell lines with different potentials for invasion and metastasis: PC1, possessing a low potential for invasion and metastasis, and PC1.0, possessing a high potential for invasion and metastasis. These two cell lines were established from the same pancreatic ductal carcinoma induced by *N*-nitrosobis (2-oxopropyl) amine in a Syrian golden hamster.[1,2] Moreover, PC1.0 cell lines were found to produce a soluble proteinaceous factor in the medium; this factor was found to induce cell dissociation and therefore we designated it the 'dissociation factor'.[3–5] We hypothesized that isolation of this factor might provide great insight into the molecular and cellular mechanisms of pancreatic cancer invasion and metastasis, and we therefore examined differences in the mRNA expression profiles of PC1 and PC1.0 using the representational difference analysis

(RDA) method. We detected five gene fragments (clones) that were expressed at higher levels in the PC1.0 cells compared with the PC1 cells.[6] We reported, in previous studies, the close association of cell dissociation with impairment of epidermal growth factor receptor signal transduction, which induces the MEK–ERK signaling pathway, resulting in disruption of the distribution of tight junctions.[7–13] However, the abovementioned dissociation factor remains to be characterized.

In the present study, we isolated a new candidate gene associated with the potential for invasion of pancreatic cancer. One of the unknown gene fragments (clone 7) detected by RDA mentioned above was revealed to encode oxysterol binding protein-related protein (ORP)-5, which is a member of the ORP family.[14,15] Oxysterol binding protein (OSBP) is a cytosolic mammalian protein that binds oxysterol ligand and interacts with Golgi membranes.[16–20] It has been reported to be involved in vesicle transport, lipid metabolism, and signal transduction.[21–28] However, the relationship between ORP5 and cancer has not been clarified.

The present study is the first to show that ORP5 is closely related to cancer invasion, and that high expression levels of ORP5 are associated with poor prognosis in human pancreatic cancer.

Materials and Methods

Cell lines and cell culture. The hamster pancreatic cancer cell lines PC1 and PC1.0, and human pancreatic cancer cell lines Capan1, Capan2, Hs700T, MiaPaCa2, and Panc1 (American Tissue Culture Collection, Rockville, MD, USA) were cultured in the recommended media supplemented with 10% fetal bovine serum (Gibco-BRL, Grand Island, NY, USA), 100 U/mL penicillin G, and 100 µg/mL streptomycin at 37°C in a humidified atmosphere of 5% CO_2 : 95% air.

cDNA library screening. Total RNA of PC1.0 was extracted using TRIzol (Invitrogen, Carlsbad, CA, USA) and treated with DNase to remove genomic DNA. Construction of the cDNA library was carried out according to the instruction manual of the ZAP-cDNA Synthesis Kit (Stratagene, La Jolla, CA, USA). Five hundred thousand plaques were thus plated, and the labeled DNA fragments were screened and detected using ECL Direct Nucleic Acid Labelling and Detection System (GE Healthcare Buckinghamshire, UK). A single positive phage was plated on a LB medium-kanamycin plate with an ExAssist helper phage and XLOLR cells (Stratagene). Plasmid DNA extraction was then carried out using a QIA filter Plasmid Maxi Kit (Qiagen, Valencia, CA, USA), and sequencing was carried out using the ABI 310 autosequencer (Applied Biosystems, Foster, CA, USA).

5′ Rapid amplification of cDNA ends. Amplification of the unknown 5′ end of the isolated novel gene was carried out according

[3]To whom correspondence should be addressed. E-mail: hdobaba@kumamoto-u.ac.jp